Journal of Southeast University (English Edition) Vol. 31, No. 1, pp. 130 - 136 Mar. 2015 ISSN 1003—7985

Calculation mode of side friction for large open caisson

Ouyang Xiaoyong[1,2,3] Zhao Wenguang[1,2] Li Jin[3] Li Song[3]

([1]School of Civil Engineering and Mechanics, Huazhong University of Science and Technology, Wuhan 430074, China)
([2]Hubei Key Laboratory of Control Structure, Huazhong University of Science and Technology, Wuhan 430074, China)
([3]CCCC Second Highway Engineering Co., Ltd, Xi'an 710065, China)

Abstract: To overcome the problems in design methodologies and construction control measures for the large open caisson, systematic research was conducted on the side friction calculation mode of the large open caisson. Based on the field monitoring data of lateral soil pressure on the side wall of the open caisson for the southern anchorage of the Maanshan Yangtze River Highway Bridge, the statistical result of the side friction under different buried depths of the cutting edge of the open caisson was back-analyzed; and the side friction distribution of the large open caisson was underlined. The analysis results indicate that when the buried depth of the cutting edge is smaller than a certain depth H_0, the side friction linearly increases with the increase in the buried depth. However, as the buried depth of the cutting edge is larger than H_0, the side friction shows a distribution with small at both ends and large in the middle. The top of the distribution can be regarded as a linear curve, while the bottom as a hyperbolic curve. As the buried depth of cutting edge increases continuously, the peak value of the side friction linearly increases and the location of the peak value gradually moves down. Based on the aforementioned conclusions, a revised calculation mode of the large open caisson is presented. Then, the calculated results are compared with the field monitoring data, which verifies the feasibility of the proposed revised calculation mode.

Key words: large open caisson; side friction; distribution diagram; calculation mode
doi: 10.3969/j.issn.1003 - 7985.2015.01.022

Open caisson has been widely used in the construction of port, bridge, mining, and water conservancy and hydropower engineering[1-3] due to less occupied area, less excavation, its convenient construction and greater bearing capacity. The side friction on the side wall of open caisson and end resistance are the two key controlling factors during the sinking. Undoubtedly, studies on the basic mechanical behavior[4-6], designing and calculating method[7-9], and construction control measure[10-12] for small and medium-sized open caissons are abundant and some of the results have been adopted by the technical code and standards of open caisson. The open caisson foundation begins to develop in a larger and deeper way. However, the existing analysis theories and design methodologies are more suitable for the design of small and medium-size open caissons.

For a long time, the distribution diagram of friction can be obtained by two approaches. The first approach is the suggestion mode offered by standard GB 50069—2002[13], which is obtained by the mechanical behavior of a large diameter pile in pile-sinking[14]. However, Wu[15] conducted a series of field tests and discovered that the side friction distribution of the open caisson is different from that of pile. For the second approach, the side friction is obtained by multiplying the lateral pressure by the external friction coefficient of the side wall of the open caisson, which is calculated by the classical active earth pressure theory. However, the soil squeezing effect of the open caisson and the repeated perturbation of the surrounding soil induced by the sinking of the open caisson are not included in the classical active earth pressure theory. More importantly, no advanced design guide or construction control technology of the deep water open caisson is proposed in practice. Hence, it is necessary to improve the existing calculation model to obtain an accurate side friction for a super-large caisson and optimize the relevant design theories.

The objective of this paper is to analyze the distribution of side friction and propose a revised calculation model for the super-large caisson. First, based on the field monitoring data of lateral pressure for the southern anchorage of the Maanshan Yangtze River Highway Bridge, the distribution of side friction on the open caisson is performed with the back analysis method. Secondly, a revised calculation mode is proposed for the side friction of the super-large open caisson. Finally, the results of the revised calculation mode are compared with the filed monitoring data to investigate its validity.

1 Distribution of Side Friction

As is known to all, the monitoring of the side friction of the open caisson is difficult, perhaps not possible, in

Received 2014-08-26.
Biographies: Ouyang Xiaoyong (1962—), male, graduate; Zhao Wenguang (corresponding author), male, doctor, professor, zhao_wenguang1037@126.com.
Foundation item: Project supported by China Communications Construction Company Limited (No. 2008-ZJKJ-11).
Citation: Ouyang Xiaoyong, Zhao Wenguang, Li Jin, et al. Calculation mode of side friction for large open caisson[J]. Journal of Southeast University (English Edition), 2015, 31(1): 130 - 136. [doi: 10.3969/j.issn.1003 - 7985.2015.01.022]

practice. Hence, the side friction is generally obtained by the back-analyzed method with the lateral pressure on the side wall of the open caisson. Then, the side friction, f_s, of the open caisson can be expressed as

$$f_s = \sigma_a \tan\delta \quad (1)$$

where σ_a is the lateral pressure on the side wall of the open caisson, which can be obtained by the measurement of the soil stress transducer; δ is the external friction angle between the soil layer and side wall of the open caisson.

As shown in Fig. 1, a number of soil stress transducers are installed on its side wall of the open caisson, which can be used to obtain the lateral pressure on its side wall. The installation of soil stress transducers is presented in Fig. 2. The statistical result of the side friction under different buried depths of the cutting edge of the open caisson

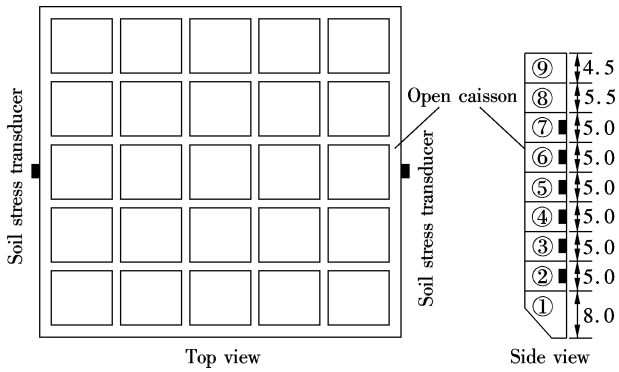

Fig. 1 Arrangement of soil stress transducers on the side wall of the open caisson (unit: m)

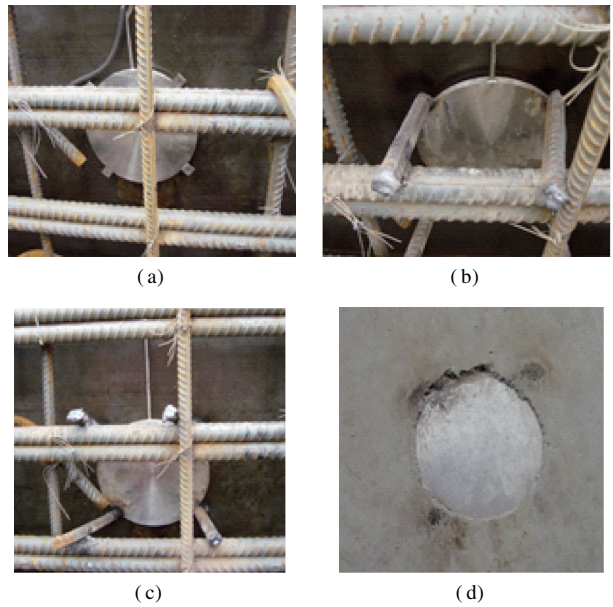

Fig. 2 Installation of soil stress transducers on the side wall of the open caisson. (a) Positioning transducer; (b) Fixed by welding; (c) Installation; (d) Demolition of the mould

is back-analyzed with the lateral pressure by Eq. (1). The friction coefficients of soil layers are listed in Tab. 1. On the basis of the side friction tendency, the variation of the side friction can be divided into two stages and the boundary of the buried depth of the cutting edge for the two stages is about 18.0 m. Figs. 3 and 4 illustrate the distributions of side friction for the two stages with different buried depths of the cutting edge.

Tab. 1 External friction angle of soil layers

Name	Elevation/m		Thickness/m	Internal friction angle ϕ/(°)	External friction angle δ/(°)		Friction coefficient μ
	Surface	Bottom			Range	Selected value	
Silt	6.5	5.65	1.15	28	9 to 14	12	0.21
Silty clay	5.65	1.79	3.86	18	6 to 9	8	0.14
Silty clay	1.79	−2.85	4.64	20	6 to 10	8	0.14
Silty sand	−2.85	−11.53	8.68	34	11 to 17	14	0.25
Fine sand	−11.53	−33.78	22.25	36	12 to 18	15	0.27
Medium sand	−33.78	−40.80	7.03	40	13 to 20	20	0.38

Notes: External friction angle $\delta = \phi/3$ to $\phi/2$; friction coefficient $\mu = \tan\delta$.

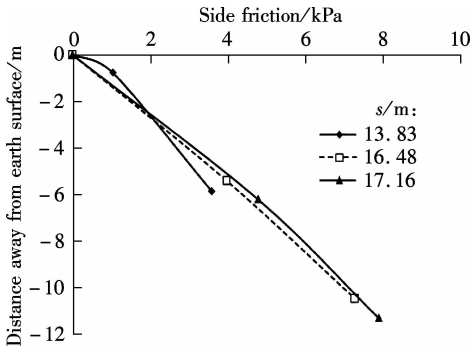

Fig. 3 Distribution of side friction under different buried depths in the first stage

For the first stage, as shown in Fig. 3, the increase in the side friction is almost linear with the increase in the buried depth of the cutting edge. However, for the second stage, the distribution of side friction presents a parabolic diagram with small at both ends and large in the middle, as shown in Fig. 4. Moreover, the distribution of the side friction in the second stage is almost linear before the side friction reaches the peak value. In terms of the increase rates of the linear parts in Figs. 3 and 4, the critical depth for the transformation of side friction distribution from linear to parabola is about 6.0 m. Fig. 4 also shows that the peak value of side friction tends to increase with the increase in the buried depth of the cutting edge, and the location of the peak value tends to move down. An explanation can be that, during the sinking, the soil close to the inside of the cutting edge will be sucked away by the suction pipe and a pressure difference will form be-

tween the inside and outside of the cutting edge. Under the pressure difference, the soil outside the cutting edge tends to flow into the inside. As a result, the soil is loose and the soil pressure decreases, and then a pressure relaxation zone will form, as shown in Fig. 5. Not coincidentally, similar regularity has also been reported by Chen et al. [3]

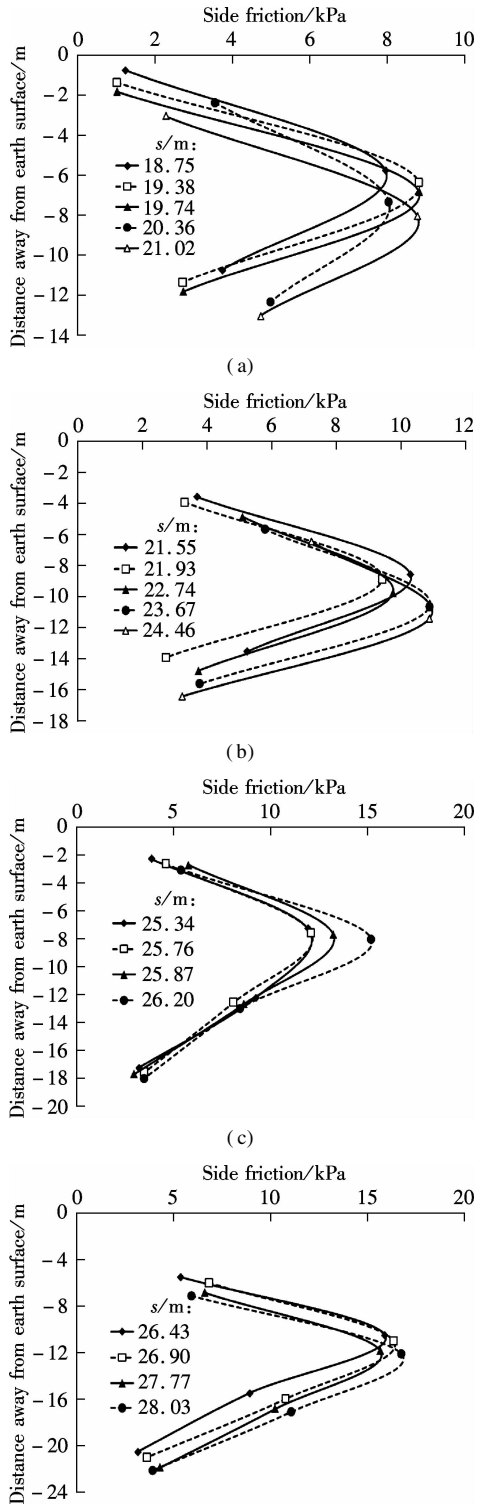

Fig. 4 Distribution of side friction under different buried depths of the cutting edge in the second stage. (a) Buried depth of 18.5 to 21.5 m; (b) Buried depth of 21.5 to 24.5 m; (c) Buried depth of 24.5 to 26.2 m; (d) Buried depth of 26.2 to 28.5 m

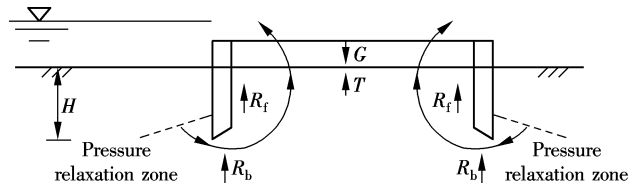

Fig. 5 Schematic of pressure relaxation zone

with the field monitoring data. In other words, the characteristic that the distribution diagram of side friction transferred from linear to parabola is widespread in large open caissons. Moreover, there is a significant difference between this kind of distribution diagram and the trapezoid distribution diagram according to standard GB 50069—2002[13].

Based on the statistics of the magnitude and location of the peak value of side friction illustrated in Fig. 4, the variations of the peak value and its location with the buried depth are presented in Fig. 6. The statistical result shows that the increase of the magnitude as well as the descent of the location of the peak value is almost linear with the increase in the buried depth of the cutting edge. In addition, it should be noted that the slope of the fitting line is 1.688, which means that the length increment of the linear upon the peak value is about 0.6 m (i.e., 1/1.688) with a 1.0 m increase in the buried depth of the cutting edge.

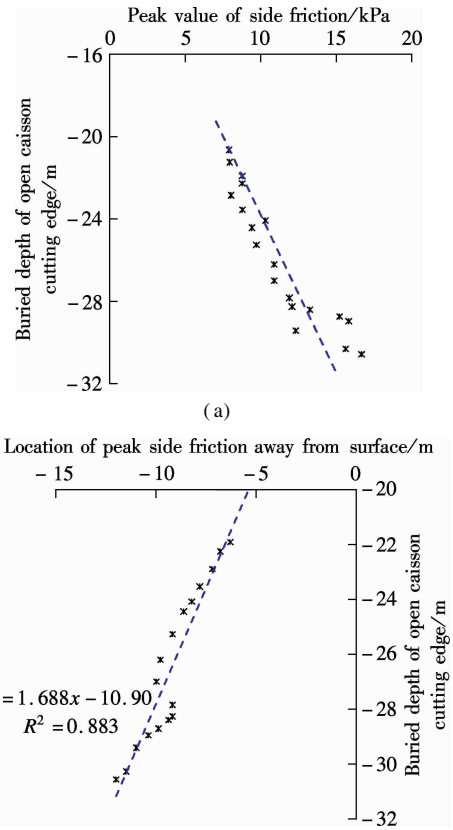

Fig. 6 Variation of side friction with the buried depth of the open caisson cutting edge. (a) Peak side friction; (b) Location of peak side friction

In order to reveal the characteristic of the side friction distribution with the buried depth of the cutting edge, all of the monitoring data shown in Figs. 3 and 4 are summarized in Fig. 7. The earth surface is selected as the zero point of the coordinate. On the whole, the distribution of this data seems to be confused and disordered without any apparent regularity. Hence, to further reveal the distribution characteristic of side friction, the data is classified into two groups, and the location of the peak value is taken as the boundary between the two groups. The monitored data upon the peak value is illustrated in Fig. 7(b), and the ground elevation is selected as the zero of the coordinate. It can be easily observed that the trend of the data almost maintains it consistently with a linear distribution, which means that the side friction maintains nearly a constant value within the original linear, with the increase in the buried depth of the cutting edge. However, the location of the peak value tends to move down and the length of the linear tends to increase. Thus, the side friction, f_s, for the linear part, which is above the peak value of side friction, can be written as

$$f_s = k_0 \gamma_m h \tan\delta_m \tag{2}$$

where k_0 is the average lateral earth pressure coefficient of the soil layers passed through by the open caisson; γ_m is the average weight of the soil layers passed through by the open caisson; h is the sinking depth of the open caisson; δ_m is the average external friction angle of the soil layers passed through by the open caisson.

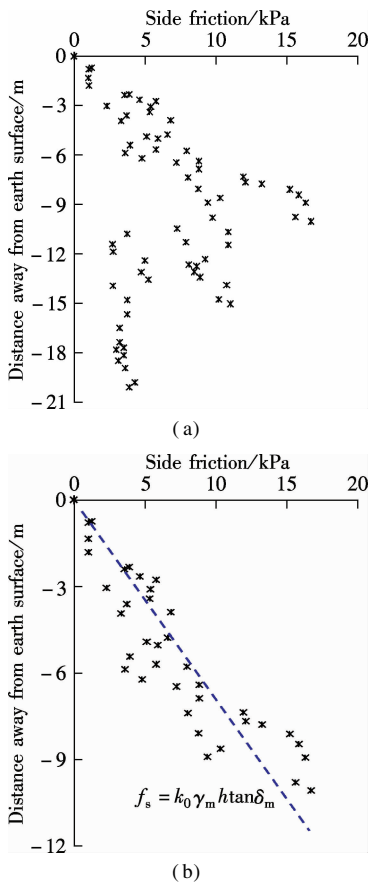

Fig. 7 Distribution of side friction. (a) All side friction; (b) Side friction with their locations above the peak value of side friction

For the monitored data below the peak value, a normalized approach is applied to each data by using Matlab. The procedures of the normalized approach are summarized as follows.

1) Fit the side friction with the Gaussian-polynomial function, and obtain the peak value, $f_{s,max}$, of the fitting curve and the corresponding depth, H_1, below the earth surface.

2) Select a field monitoring data, f_s, as the target value and the corresponding depth is h, and then calculate the objective function as follows:

$$\eta = \frac{f_s - f_{s,max}}{f_{s,max}} \tag{3}$$

where $f_{s,max}$ is the fitting result corresponding to f_s.

3) Build a rectangular coordinate system with the y-axis of the $(f_s - f_{s,max})/f_{s,max}$ and the x-axis of the perpendicular distance $(h - H_1)$ away from the location of the peak value, and mark the result obtained by Eq. (3) in the coordinate system.

Based on the procedures mentioned above, each monitored piece of data below the peak value is processed and depicted in Fig. 8. The location of the peak value is selected as the zero point of the coordinate. It can be observed from Fig. 8 that the variation trend of $(f_s - f_{s,max})/f_{s,max}$ with the $(h - H_1)$ is relatively consistent, which means that the buried depth of the cutting edge almost has no effect on the value of $(f_s - f_{s,max})/f_{s,max}$. Moreover, the relationship of the $(f_s - f_{s,max})/f_{s,max}$ and $(h - H_1)$ can be well fitted by a hyperbolic function as follows:

$$\frac{f_s - f_{s,max}}{f_{s,max}} = \frac{h - H_1}{(h - H_1) - 4} \tag{4}$$

where H_1 is the location of the peak value below the earth's surface and the meanings of the other notations are the same as the former.

In conclusion, when the buried depth of the cutting edge

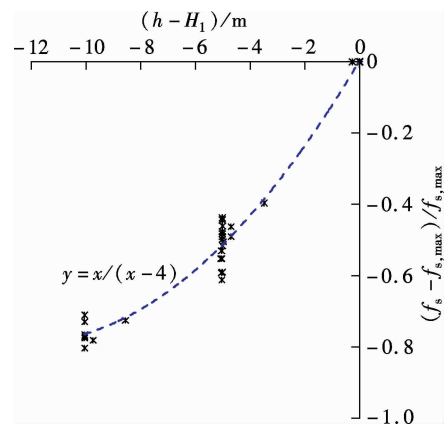

Fig. 8 Distribution of side friction below the peak value

of the open caisson is smaller than a certain depth H_0 ($H_0 \approx 6.0$ m, for the open caisson in the southern anchorage of the Maanshan Yangtze River Highway Bridge), the side friction linearly increases with the increase in the buried depth of cutting edge. However, as the buried depth of cutting edge is larger than H_0, the side friction shows a distribution diagram with small at both ends and large in the middle, the top of the distribution can be regarded as linear curve, while the bottom as hyperbolic curve. As the buried depth of the cutting edge of the open caisson increases continuously, the peak value of the side friction linearly increases and the location of the peak value gradually drops.

2 Revision of Calculation Mode for Side Friction

In standard GB 50069—2002[13], the calculation mode for the side friction during the sinking is illustrated in Fig. 9. Clearly, the trapezoid diagram of the side friction cannot reflect the fact that the peak value increases gradually with the buried depth of cutting edge and the location of the peak value gradually moving down. More importantly, the trapezoid diagram is significantly different from the parabola diagram commonly observed by field monitoring. Hence, the calculation mode in GB 50069—2002[13] is not suitable for the large open caisson.

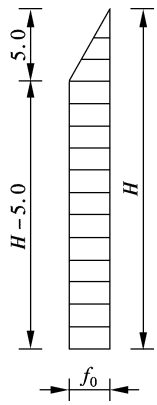

Fig. 9 The calculation mode of side friction in GB 50069—2002[13] (unit: m)

Except for the calculation mode in GB 50069—2002[13], Chen et al.[3] proposed a calculation mode, and the corresponding mathematical expressions are as follows:

$$\left.\begin{aligned} \sigma_f &= \frac{h}{H_1} f_0 && h < H_1 \\ \sigma_f &= f && H_1 \leqslant h < H_2 \\ \sigma_f &= f_0\left(1 - \frac{1}{3}\,\frac{h - H_2}{H - H_2}\right) && h \geqslant H_2 \end{aligned}\right\} \quad (5)$$

where H_1 is the location of the peak value below the earth surface and the recommendation value is 8 to 12 m in Ref. [3]; f_0 is the unit maximum side friction, which is related to some parameters, such as the soil properties and the buried depth of the cutting edge; H_2 is the lower bound depth where the side friction reaches the maximum value f_0 and will not change with the buried depth of the cutting edge, and the recommendation value of $(H_2 - H_1)$ is 1.0 to 5.0 m in Ref. [3]; h is the calculation depth.

However, the fact that the peak value increases gradually with the buried depth of the cutting edge and the location of the peak value gradually moving down is not considered in the calculation mode presented by Chen et al.[3], even though the parabola distribution characteristic of side friction has been considered. As a result, the discrepancy between the calculated result and field monitoring data is great. Thus, it is necessary to propose a revised calculation mode for the large open caisson. On the basis of the distribution characteristic of side friction presented in the preceding section, a revised calculation mode of the large open caisson will be focused on in the following subsection.

As previously mentioned, when the buried depth of the cutting edge of the open caisson is smaller than a certain depth H_0, side friction linearly increases with the increase in the buried depth of the cutting edge, as shown in Fig. 10(a). However, as the buried depth of the cutting edge is larger than H_0, the side friction shows a distribution diagram with small at both ends and large in the middle, the top of the distribution can be regarded as linear, while the bottom as hyperbolic, as shown in Fig. 10(b). Thus, the following piecewise function can be proposed to describe the distribution characteristic of the side friction:

$$f_s = \begin{cases} k_0 \gamma_m h \tan\delta_m & H \leqslant H_0 \\ f_{s,\max}\left[\dfrac{h - H_1}{(h - H_1) + C} + 1\right] & H \geqslant H_0 \end{cases} \quad (6)$$

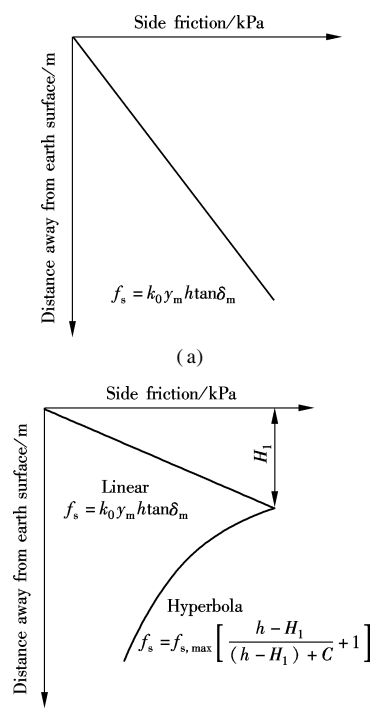

Fig. 10 The revised calculation mode of side friction. (a) $H < H_0$; (b) $H > H_0$

where h is the depth and has a negative sign for the subsurface. H_0 is the critical depth for the distribution of the side friction turning from linear to parabolic; generally, $H_0 = 6.0$ to 8.0 m; $H_0 = 6.0$ m for the project relied upon in this study and $H_0 = 7.0$ m for the field monitoring data in Ref. [3]. H_1 is the location of the peak value of side friction. As shown in Fig. 10, H_1 can be obtained by the mathematical expression as follows:

$$H_1 = k(H - H_0) + H_0 \tag{7}$$

where k is the variation coefficient for the location of peak side friction. The reduction proportional relationship between the decline of the peak side friction location and the increment of the buried depth can be directly characterized by the value of k. $k = 0.6$ for the project relied upon in this study and $k \approx 1.0$ for the field monitoring data in Ref. [3]. $f_{s,\max}$ is the peak side friction and it can be written as

$$f_{s,\max} = k_0 \gamma_m H_1 \tan\delta_m \tag{8}$$

Clearly, the revised calculation mode for the side friction of caisson defined by Eq. (6) can not only reflect the distribution with small at both ends and large in the middle, but also effectively consider the characteristic that the peak value of the side friction increases gradually with the buried depth of the cutting edge and the location of the peak value gradually moves down. Fig. 11 presents the comparison between the side friction empirically estimated by Eq. (6) and the field monitoring data, while the values of the corresponding parameters have been listed in previous section. As can be seen, the distribution of the data is almost around the oblique line of 45°, which means that the estimated f_s agrees well with the field monitoring data (coefficient of determination $R^2 = 0.917$ for the southern anchorage of the Maanshan Yangtze River Highway Bridge and $R^2 = 0.936$ for the engineering in Ref. [3]). Hence, the feasibility of the proposed revised calculation mode is verified.

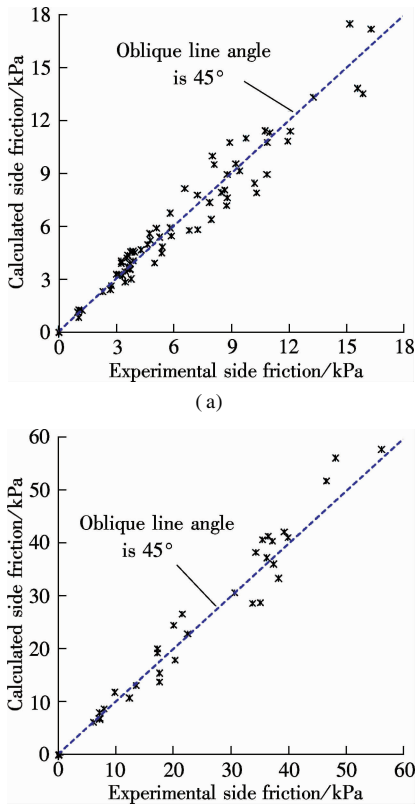

Fig. 11 Comparison between the side friction predicted by Eq. (8) and field monitoring data. (a) Field monitoring data in this paper; (b) Field monitoring data in Ref. [3]

3 Conclusion

In this study, the side friction distribution of the large open caisson is underlined with the field monitoring data of the southern anchorage of the Maanshan Yangtze River Highway Bridge. Meanwhile, a revised calculation mode of the large open caisson is proposed. From this investigation, the following conclusions can be drawn.

When the buried depth of the cutting edge of the open caisson is smaller than a certain depth H_0, the side friction linearly increases with the increase in the buried depth of cutting edge. However, when the buried depth of the cutting edge is larger than H_0, the side friction shows a distribution with small at both ends and large in the middle. The top of the distribution can be regarded as linear, while the bottom as hyperbolic. As the buried depth of the cutting edge of the open caisson increases continuously, the peak value of the side friction linearly increases and the location of the peak value gradually moves down. On the basis of these conclusions, a revised calculation mode of the large open caisson is presented. The feasibility of the proposed revised calculation mode is verified through analyzing the results obtained from the revised calculation mode and the field monitoring data.

References

[1] Pantouvakis J, Panas A. Computer simulation and analysis framework for floating caisson construction operations [J]. *Automation in Construction*, 2013, **36**: 196 – 207.

[2] Gerolymos N, Gazetas G. Development of Winkler model for static and dynamic response of caisson foundations with soil and interface nonlinearities [J]. *Soil Dynamics and Earthquake Engineering*, 2006, **26**(5): 363 – 376.

[3] Chen X P, Qian P Y, Zhang Z Y. Study on penetration resistance distribution characteristic of sunk shaft foundation [J]. *Chinese Journal of Geotechnical Engineering*, 2005, **27**(2): 148 – 152. (in Chinese)

[4] Chiou J, Ko Y, Hsu S, et al. Testing and analysis of a laterally loaded bridge caisson foundation in gravel [J]. *Soils and Foundations*, 2012, **52**(3): 562 – 573.

[5] Zhong R, Huang M. Winkler model for dynamic response of composite caisson-piles foundations: lateral response [J]. *Soil Dynamics and Earthquake Engineering*, 2013, **55**: 182 – 194.

[6] Zafeirakos A, Gerolymos N, Drosos V. Incremental dy-

namic analysis of caisson-pier interaction [J]. *Soil Dynamics and Earthquake Engineering*, 2013, **48**: 71 - 88.
[7] Varun, Assimaki D, Gazetas G. A simplified model for lateral response of large diameter caisson foundations—Linear elastic formulation [J]. *Soil Dynamics and Earthquake Engineering*, 2009, **29**(2): 268 - 291.
[8] Tanimoto K, Takahashi S. Design and construction of caisson breakwaters-the Japanese experience [J]. *Coastal Engineering*, 1994, **22**(1 - 2): 57 - 77.
[9] Kirkgoz M S, Mengi Y. Design of a caisson plate under wave impact [J]. *Ocean Engineering*, 1987, **14**(4): 275 - 283.
[10] Hu S, Wang H, Fan J. Construction process control of large extra caissons [J]. *Tsinghua Science & Technology*, 2005, **10**(3): 359 - 363.
[11] Abdrabbo F M, Gaaver K E. Applications of the observational method in deep foundations [J]. *Alexandria Engineering Journal*, 2012, **51**(4): 269 - 279.
[12] Pantouvakis J, Panas A. Computer simulation and analysis framework for floating caisson construction operations [J]. *Automation in Construction*, 2013, **36**: 196 - 207.
[13] The Ministry of Construction of PRC. GB 50069—2002 Structural design code for special structures of water supply and waste water engineering [S]. Beijing: China Building Industry Press, 2002. (in Chinese)
[14] Vesic A S. Tests on instrumented piles, Ogeechee River site [J]. *Journal of Soil Mechanics & Foundations Divison*, 1970, **96**(2): 561 - 584.
[15] Wu M B. Retaining structure of large open caisson [J]. *Chinese Journal of Geotechnical Engineering*, 1994, **16**(1): 86 - 92. (in Chinese)

大型沉井侧壁摩阻力计算模型

欧阳效勇[1,2,3] 赵文光[1,2] 李 进[3] 李 松[3]

([1] 华中科技大学土木工程与力学学院, 武汉 430074)
([2] 华中科技大学控制结构湖北省重点实验室, 武汉 430074)
([3] 中交第二公路工程局有限公司, 西安 710065)

摘要:为了克服大型沉井设计和施工控制中存在的问题,对大型沉井侧壁摩阻力的计算模式进行了研究. 根据马鞍山长江大桥南锚碇沉井侧壁土压力的现场监测数据,反推出不同下沉深度条件下沉井侧壁摩阻力的统计结果,并研究了大型沉井下沉期侧壁摩阻力的分布特征. 分析结果显示:当沉井下沉深度小于某一特定深度 H_0 时,井壁侧阻力基本上随着入土深度呈线性增长;而当沉井刃脚入土深度大于 H_0 时,沉井侧壁摩阻力分布呈现上下小、中间大的分布,上部可近似为线性段,下部则近似为双曲线段;而且随着沉井入土深度的不断增加,沉井侧壁摩阻力峰值基本呈线性增长,且峰值发生的位置也逐渐下移. 最后,建立了一种大型沉井侧壁摩阻力的修正计算模式. 与现场实测数据的对比结果表明,所提出的修正计算模式是可行的.

关键词:大型沉井;侧摩阻力;分布图式;计算模型
中图分类号:TU74